GEANT-4 SIMULATIONS OF SECONDARY POSITRON EMITTED CARBON ION BEAMS

E. Syresin#, V. Volnyh, Joint Institute for Nuclear Research, Dubna, 141980, Russia

Abstract

The radioactive ion isotopes $^{11}C^{6+}$, $^{10}C^{6+}$ and others are produced at interaction of primary carbon ion beam with target. These isotopes can be applied for Positron Emission Tomography (PET). The projectile-fragmentation method is used for the production of radioactive isotopes. The intensity of radioactive ion beam is defined by the optimal target thickness and available longitudinal and transverse acceptances of transport channel. A growth of target thickness permits to improve the production rate of the radioactive ion beams, however it increases the energy and angle spreads of secondary ions and finally it gives a reduction of number of the radioactive ions which can be transported to the PET camera. The GEANT-4 simulations related to formation of the $^{11}C^{6+}$ secondary ion beams at interaction with different targets are discussed.

SECONDARY CARBON ION BEAMS

Heavy-ion cancer therapy using a ^{12}C-beam has been carried out at several hospital centres in the world. A beam intensity of $2\cdot10^9$ has routinely been used for cancer therapy. The extracted ion intensity will be reduced to 10^8 pps in the scanning irradiation scheme realized in near future with carbon beams. The application of positron emitter beam such as ^{11}C, for cancer treatment gives great advantage because the shape of an irradiated errea in the human body can be detected directly by PET. The formation of positron emitter beams is actually to avoid the irradiation treatment errors near the critical organs. PET permits to obtain a dose distribution with a high accuracy in an online patient treatment mode.

The projectile-fragmentation method is used for production of $^{11}C^{6+}$ positron emitted beam at interaction of the primary beam with the production target [1]. The parameters of the primary and secondary beams are given in Table 1. The axial emittance of the primary beam corresponds to ε_z=5.9π·mm·mrad, the target β_z-function is equal to β_z=3m, the size of primary beam $^{12}C^{6+}$ is of $2\sigma_z=\pm 4.2$ mm, the ion angles corresponds to $2\sigma'_z=\pm 1.4$ mrad. The primary beam has the Gaussian distribution at the entrance of the production target. The radial emittance of primary beam is equal to ε_r= 6.8 π·mm·mrad. The radial size of the primary beam corresponds to $2\sigma_r=\pm 4.5$ mm and ion radial angle spread is of $2\sigma'_r=\pm 1.5$ mrad, the target radial β_r -function is equal to β_r=3 m. Average primary ion energy is equal to 400 MeV/u and energy spread corresponds to $\Delta W/W$ (± 2σ)=±0.097%. The particle distribution of $^{12}C^{6+}$ ions versus its energy is shown on Fig.1.

#syresin@nusun.jinr.ru

Table 1: Parameters of Primary and Secondary Carbon Ion beams

Primary carbon ion energy, MeV/u	400
Relative energy spread (±2σ),%	±0,097
Target beta-functions, β_z/β_r, m	3/3
Beam emittances, $\varepsilon_z/\varepsilon_r$, π·mm·mrad	5,9/6,8
Beam sizes, $2\sigma_z/2\sigma_r$, mm	±4,2/±4,5
Angle spreads, , mrad	±1,4/±1,5
Channel vertical angle acceptance, mrad	13
Channel longitudinal acceptance %	±2.6
Carbon target thickness, mm	27
Production conversion efficiency in $^{11}C^{6+}$ ions. %	2,9
Production and collection conversion efficiency, %	1,3
Secondary ion average energy, MeV/u	346,5
Secondary ion relative energy spread, (±2σ)%	±1,2
Angle spread, $2\sigma'$, mrad	±27,8

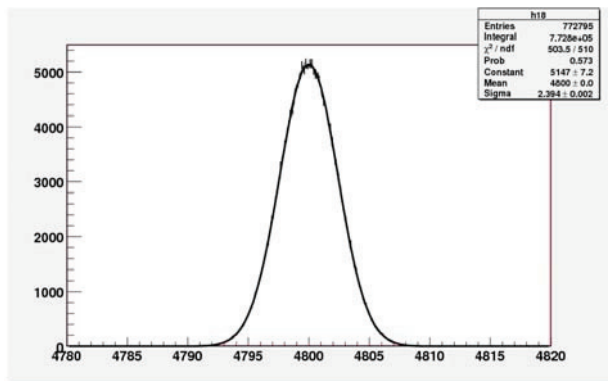

Figure 1: Total kinetic energy distribution of primary $^{12}C^{6+}$ ion beam.

The production rates and parameters of the $^{11}C^{6+}$ ion beam are simulated by the GEANT-4 code [2]. The number of the primary ions $^{12}C^{6+}$ at the target entrance corresponds to 10^6 particles in GEANT 4 simulations. The carbon target at a thickness of 27 mm provides deceleration of the primary ions from energy 400 MeV/u to 346.5 MeV/u (total ion kinetic energy is of 3.812 GeV) (Fig.2). The kinetic energy spread of secondary ions is equal to $\Delta W(\pm\sigma)$=24.1 MeV, that corresponds to the relative energy spread of $\Delta W/W(\pm 2\sigma)$ = ±1.2%. It is one order magnitude larger the energy spread of the primary carbon beam.

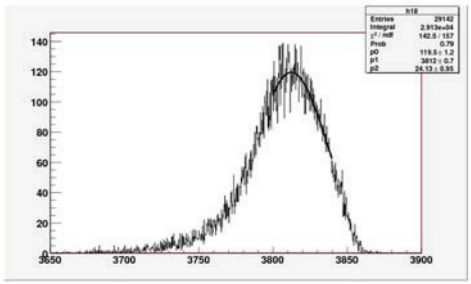

Figure 2: Total kinetic energy distribution of secondary $^{11}C^{6+}$ ion beam.

The size of the radioactive carbon beam at the target exit practically corresponds to initial size of the primary beam (Fig.3). However the angle spread of $\sigma'_z == \pm 13.9$ mrad is larger by 20 times for the radioactive carbon beam (Fig. 4) comparing with the initial angle spread of the primary beam.

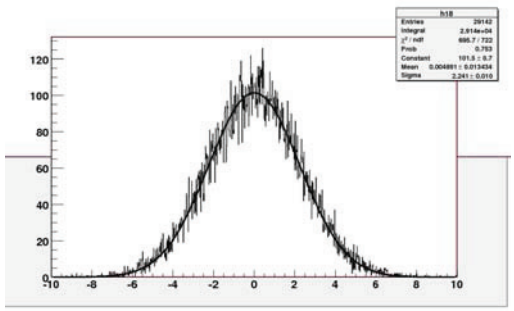

Figure 3: Distribution of $^{11}C^{6+}$ ions versus vertical coordinate.

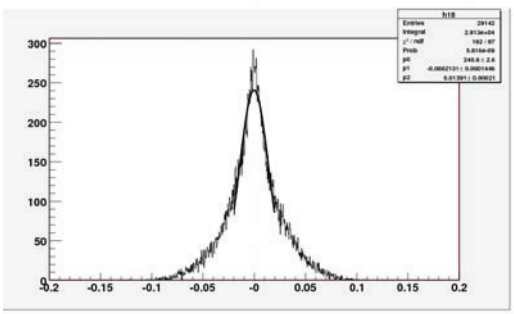

Figure 4: Distribution of $^{11}C^{6+}$ ions versus vertical angle.

The production efficiency of the positron-emitted isotopes $^{11}C^{6+}$ is equal to 2.9%. The vertical angle acceptance of the transport channel is given to 13 mrad. It leads to production-collection rate of the secondary ions $^{11}C^{6+}$ of 1.3%. An optimal production-collection rate is defined by the target thickness.

The formation of the radioactive beams in the targets of different thickness is presented on Fig.5-Fig.6. The relative energy spread of the primary ions is linearly increased at small target thickness caused by the energy straggling (Fig.5). The energy spread of secondary beam is fast increased with target thickness (Fig.5). This value is larger by one order of magnitude comparing with the energy spread of the primary ion beam at the target thickness larger 50 mm (Fig.5). The energy spread of the secondary beam is 3 times larger than primary one at a low target thickness of 15 mm. The high energy spread of secondary beam at a large target thickness restricts the collection efficiency of the secondary ions caused by the transport channel longitudinal acceptance. The angle spread of secondary ions (Fig.5) is several times larger comparing with the angle spread of the primary ions. The large angle spread of the secondary ions restricts their collection efficiency caused by the transport channel vertical angle acceptance.

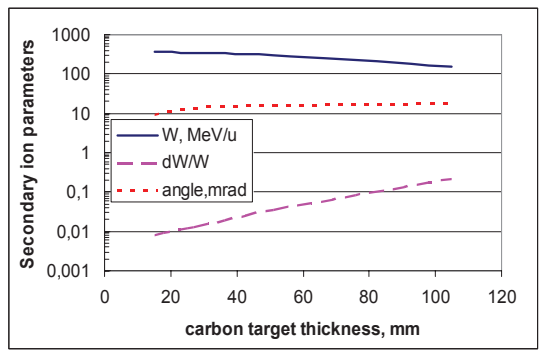

Figure 5: Secondary $^{11}C^{6+}$ ion parameters versus of carbon target thickness.

The secondary ion production rate is linearly increased at carbon target thickness smaller 50 mm (Fig.6). A saturation of the secondary ion production rate is related to a reduction of the primary ion transition efficiency through the target at its thickness larger 50 mm (Fig. 6). The given transport channel vertical angle acceptance 13 mrad and longitudinal acceptance ±2.6% became to a reduction of the production-collection rate caused by the secondary ion losses at a large ion energy and angle spreads. An optimal carbon target thickness corresponds to 50 mm (Fig.6) at which the maximal production-collection rate is equal to 2% for given vertical angle and momentum acceptances. The production-collection rate is small at a target thickness less than 30 mm caused by a low production rate (Fig. 6). The collection efficiency is reduced at a target thickness larger 50 mm caused by a large energy and angle spreads of the secondary ions (Fig.5 and Fig. 6).

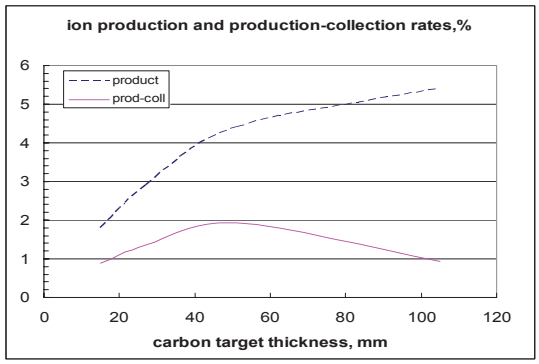

Figure 6: Secondary ion production and production-collection rate versus carbon target thickness.

The production-collection rates of the secondary ions $^{11}C^{6+}$ are given in Fig.7 at different thickness of the beryllium targets and initial energy of the primary ions of 350 MeV/u. The transport channel vertical angle acceptance of 13 mrad and the longitudinal acceptance of ±2.6% became to reduction of the production – collection rate from 2.4% to 0.56% (Fig.7) caused by the large secondary ion energy spread of $\Delta W/W(\pm 2\sigma) = \pm 4.8\%$ and angle spread of $\sigma'_z = \pm 39$ mrad.

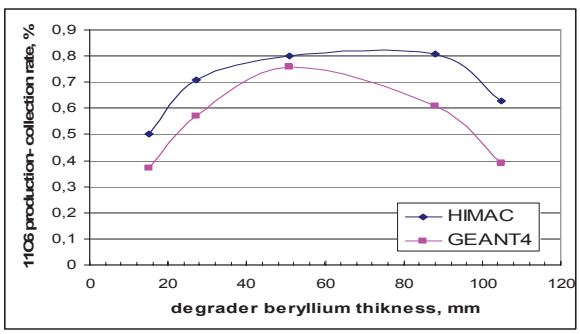

Figure 7: Dependence of production-collection rate of ^{11}C ions versus beryllium target thickness.

The simulation results have a good agreement with HIMAC experiment dates [1] (Fig.7). The production rate of ^{11}C ions corresponds to 4.6% at beryllium target thickness 88 mm. The ^{11}C ion energy and angle spreads are increased at a target thickness growth. As result, the production-collection rate of ^{11}C ions is reduced to 0.4%, caused by angle and momentum acceptances of the transport channel. The energy spread of secondary ions corresponds to $\Delta W/W(\pm 2\sigma) = \pm 10\%$ and their angle spread is equal to f $\sigma'_z = \pm 47$ mrad.

The beryllium target provides production-collection rate of 0.7% at an optimal thickness 50 mm and given above acceptances. Accordance to the HIMAC experience [1] a ^{11}C production-collection rate of 0.3% is required to realize a reasonable treatment time at a primary ^{12}C ion beam intensity of $2 \cdot 10^9$ pps.

PRIMARY POSITRON-EMITTED CARBON ION BEAMS

To increase the intensity of primary radioactive carbon ion beams $^{11}C^{6+}$ by two orders of magnitude, the ISOLDE scheme was proposed in [3]. An advantage of primary radioactive ^{11}C ion beams is the higher space resolution at PET tomography in compare to secondary radioactive beams produced in the Projectile Fragmentation Method.

In the ISOLDE scheme the ^{11}C-isotope can be produced through the nuclear reaction ^{14}N (p,α)^{11}C in the target chamber filled with N_2 gas and 5% of H_2 at initial pressure of about 20 bars [3]. The proton beam from the 18 MeV cyclotron allows to get the $^{11}CH_4$ molecules at activity of 0.06 Ci ($4 \cdot 10^{12}$ atoms of ^{11}C) with the proton beam current of 20 μA. A Porapac cryogenic trap is used for separation of iced radioactive methane $^{11}CH_4$ from N_2 gas pumped away from trap. After stopping the flow of the target gas, the cryogenic system raises the temperature and the radioactive methane is passed into a reservoir tank. The total time for its separation is 3 minute at collection efficiency of 95%.

After separation procedure the $^{11}CH_4$ methane molecules are loaded into an ion source. The radioactive methane is used a working gas in the ion source. The conversion efficiency of methane molecules in to the ions $^{11}C^{4+}$ corresponds to $\xi = 17\%$ in the JINR Electron string ion source (ESIS) [4-5]. The present number of extracted primary radioactive $^{11}C^{4+}$ ions per pulse is equal to $4 \cdot 10^9$ in the ESIS source. Now a new ESIS with $^{11}C^{4+}$ ion intensity of $6 \cdot 10^9$ particles per pulse .is under construction in JINR.

The primary $^{11}C^{4+}$ ions are injected in the linear accelerator and then in the carbon synchrotron. The number of the primary $^{11}C^{6+}$ ions accelerated in the synchrotron corresponds to $2 \cdot 10^9$ per injection pulse. The number of primary $^{11}C^{6+}$ ions extracted for scanning irradiation is 10^8 pps.

REFERENCES

[1] M. Suda et al., EPAC'00, p.2554 (2000); http://www.JACoW.org.

[2] www.slac stanford edu/comp/physics/geant4/ slac_physics_lists/micro/physlistdoc.html.

[3] S. Hojo et al., Production of ^{11}C-beam for particle therapy, Paris, ID:0045 (2004).

[4] E.D. Donets et al, HIAT'09, E1 (2009); http://www.JACoW.org.

[5] D.E. Donets et al., J. of Appl. physics 3, (2010), 34.